Seismic assessment of masonry structures – Experimental program

J. Molina, Y. Le Pape, P. Pegon
ELSA, IPSC, Joint Research Centre, European Commission, I-21020 Ispra (VA) Italy

ABSTRACT: This paper presents an overview of the experimental work performed in the framework of the SEISPROTEC project dealing with the failure of masonry walls. Two types of related tests are performed: structural walls loaded in shear and wallettes loaded bi-axially.

1 INTRODUCTION

The Joint Research Centre of the European Commission launched in 1999 an institutional research project on seismic assessment of masonry structures (SEISPROTEC), which is focussed on the protection of cultural heritage structures (Pinto et al. 2001).

The objective of the experimental work is to provide an in-depth study of the in-plane behaviour of masonry walls. It is strongly connected with a numerical work that is performed in parallel and presented in an accompanying paper (Le Pape et al. 2001).

The materials used in the project - solid bricks and a poor quality mortar - hydraulic lime and sand in volumetric ratio 1:3 – are representative of ancient masonry. Two types of tests are performed (see Fig. 1) corresponding to two different modelling levels.

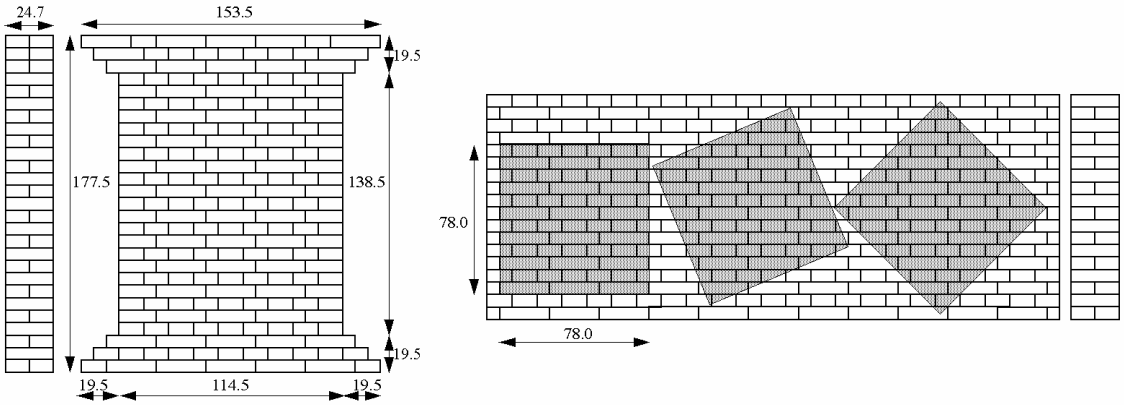

Figure 1: Dimension of the shear walls and of the wallettes.

(i) Shear walls - height to width ratio around 1.2 - built in English bond are tested under cyclic shear loading and constant vertical force. The rotation of the upper-beam is prevented. Such conditions are indeed realistic of masonry walls susceptible to fail in shear during a seismic event. This corresponds to the structural modelling level.

(ii) Square large assemblage/*walettes* (80x80cm) orientated along different directions are tested under a monotonic/cyclic homogeneous biaxial stress state. The direction of anisotropy, together with the loading paths, is to be chosen with respect to what occurs in the shear wall. This corresponds to the meso-scale (almost homogeneous) modelling level.

The paper will present both setups together with the experimental results already obtained.

2 STRUCTURAL SHEAR WALL

2.1 Test setup and instrumentation

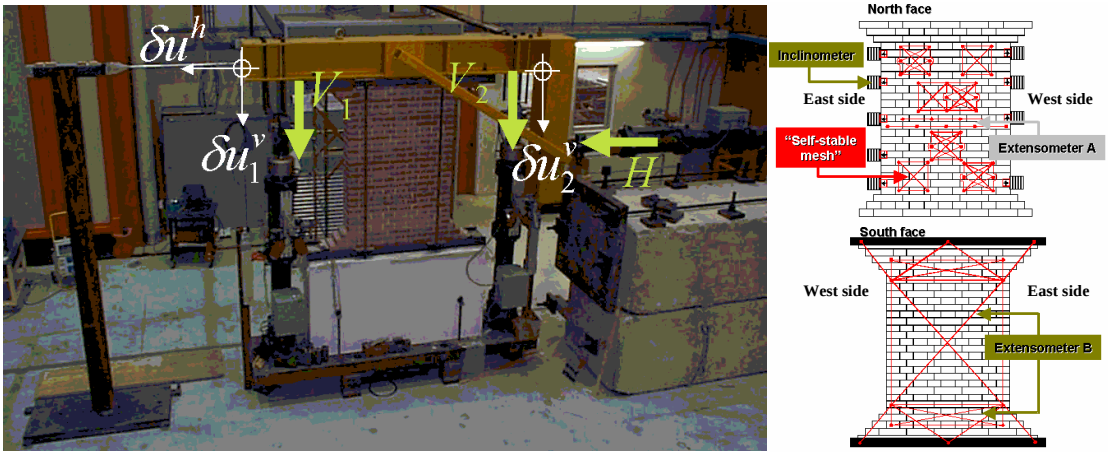

Figure 2: Test setup and instrumentation for the wall.

The loads are applied through a steel rigid upper-beam (see Fig. 2). The vertical displacements of the right and the left side of the beam are controlled in such a way they remain equal and the sum of the left and right forces remains constant, equal to a prescribed resultant. Note that the beam is free to move vertically. In order to limit the forces required to block the rotation of the beam, the horizontal force is applied at the level of the centre of gravity of the wall. The horizontal displacement is prescribed during the test.

In order to avoid a dangerous collapse in the case of instability of the wall with respect to the vertical load, the control of the vertical pistons is made in displacement and the target of both of them is computed by one processor only, which takes into account the measured forces and displacements, and a specified safe maximum displacement velocity.

The instrumentation has been conceived in order to feed back the numerical activity (see Fig. 2). Therefore, extensometers of various dimensions have been placed upon one surface of the wall (North face) so as to obtain accurate measurement at various scales. The other face (South face) of the wall is left to the investigation of the structural response in order to discriminate the failure mode (shear, sliding…). As far as the north face is concerned, two parallel objectives are pursued: the calibration of the numerical models by back-analysis and the knowledge of homogenized stress/strain history that will be used as inputs to the later tests of large assemblages. The stress/strain field homogeneous on average cannot be obtained as a complete pattern on the wall. However, it is necessary to ensure several points (or "cells") of measurement to obtain an adequate discrete field. Two types of self-stable meshes of extensometers have been adopted for obtaining cell homogenised results: a mesh of ten extensometers - the four external sides and the main diagonal control the state of average strain on a large cell including four brick layers, the four additional smaller diagonals allow to get some strain state measures on a smaller, basic cell including two brick layers– and a simplified mesh of six extensometers. Local measurements of the mechanical behaviour of the mortar joints are also performed to detect the loss of bond due to shear/tensile degradation process in the joints or the occurrence of brick cracks. It has been proposed to make a simple instrumentation of two horizontal lines in the central part of the wall. Some inclinometers have been distributed along the sides of the wall in order to measure the in-plane rotation of the external bricks.

2.2 Results observed during the first test.

The first test (SW1) has been performed at the end of December 2000. It was mainly a verification test for the loading setup and instrumentation, and the base of definition of the more intensive testing campaign that is currently running.

2.2.1 Loading

The quasi-static SW1 test has been performed with a constant vertical load and a controlled cyclic horizontal displacement of the upper-beam.

The value of the vertical load has been determined in order to obtain an average vertical pressure of 0.6 [MPa]. Such value is believed to be relevant of traditional masonry buildings. This stress level is equivalent to a vertical load of 150 [kN]. Due to the asymmetry of the loading-rig for that test (its barycentre was positioned at the east of the wall) with respect to the vertical axis of symmetry of the wall, the initial equality of the forces within the two vertical hydraulic jacks was not ensured. Therefore, an external counterbalance has been added so that the in-plane moment almost vanishes. However, it shall be emphasised that the load cells controlling the forces within the vertical pistons measured a differential loading close to 20 [kN]. This was probably due to the lack of symmetry of the wall itself.

The controlled horizontal displacement of the upper-beam follows a cyclic history with an increasing of the peak-to-peak amplitude. The set of the horizontal peak displacements contains the following values (values given in [mm], followed by an integer written between parenthesis indicating the number of the displacement peak): -0.7(1), 1.4(2), -3.2(3), 3.9(4), -5.4(5), 6.3(6), -7.4(7), 8.2(8), -9.3(9), 10.1(10) and finally -20.6(11).

2.2.2 Structural behaviour

Up to the fourth cycle, the hysteretic behaviour is not strongly marked. Later the horizontal behaviour becomes highly non-linear and dissipative (see Fig. 3). It should be emphasised that the starting point of this non-linear behaviour matches with the occurrence of the first heard cracking sonic emissions. The ultimate horizontal loads are recorded for the 5th and the 6th peaks with some corresponding values respectively of –54 [kN] and +56 [kN]. The first visible cracks were observed before the 6th peak. The following cycles exhibit some high hysteretic behaviour. The minimum residual horizontal loads are equal to +47 [kN] (10th peak) and –48 [kN] (11th peak), i.e. a decrease of 16% (resp. 11%) with respect to the recorded ultimate load. These residual loads should be used as the limit design horizontal load (design strength). The observed substantial displacements (up to 20 [mm]) pointed out the unexpected ductility of the wall. No further trial up to some larger displacements was attempted in order to avoid the risk of sudden collapse with loss of the instrumentation. The loss of stiffness indicates some significant cyclic damage. Once the peak load is overtaken, the instantaneous unloading stiffness (immediately following the peak) is rather high. A short unloading (roughly linear) phase is followed by a sudden drop of stiffness that decreases slowly and thus creates some large hysteretic loops (see Fig. 3). A change of stiffness is also observed while crossing the displacements axis.

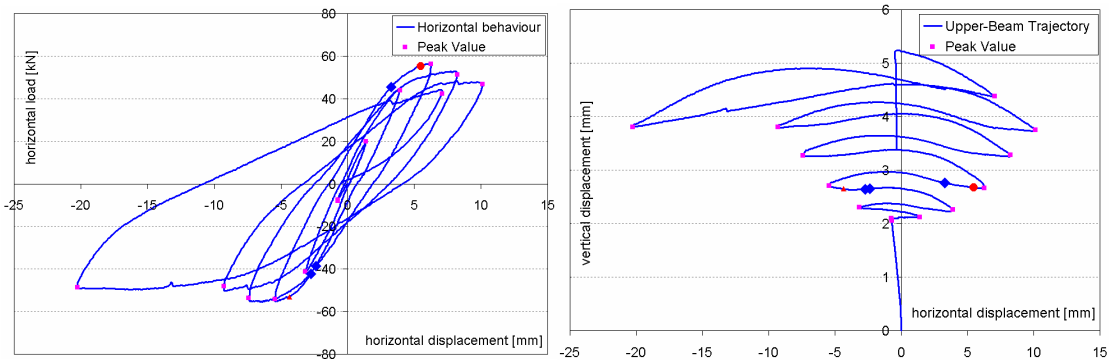

Figure 3: Horizontal load and vertical contraction versus horizontal displacement.

The vertical resultant is kept constant (loading: 150 [kN]) after a linear increasing ramp. As mentioned previously, a difference around 20 [kN] has to be emphasised between the two vertical jacks, apparently due to an asymmetric behaviour of the specimen. The recorded vertical displacements of the upper-beam are almost equal all along the test indicating that the rotation was perfectly prevented. As a general trend, the vertical displacement increased from 2.1 [mm] at the end of the vertical pre-loading to reach a maximum value of 5.3 [mm]. The value of the vertical displacement induced by the vertical pre-loading is excessive and reveals the presence of important imperfections so that it is suspected that the large amount of vertical displacement may be

induced by some closing of the initial defects and not to the intrinsic deformability of the constitutive materials. It should be emphasised that the maximum vertical displacement was not obtained for a peak of horizontal displacement. The observation of the trajectory of the upper-beam (see Fig. 3) shows that a representative evolution of the vertical displacement from horizontal displacements peak-to-peak is not monotonic: some vertical expansion always follows some vertical contraction. The position of the inflexion point (i.e. the value of the horizontal displacement for which this change occurs) is not constant.

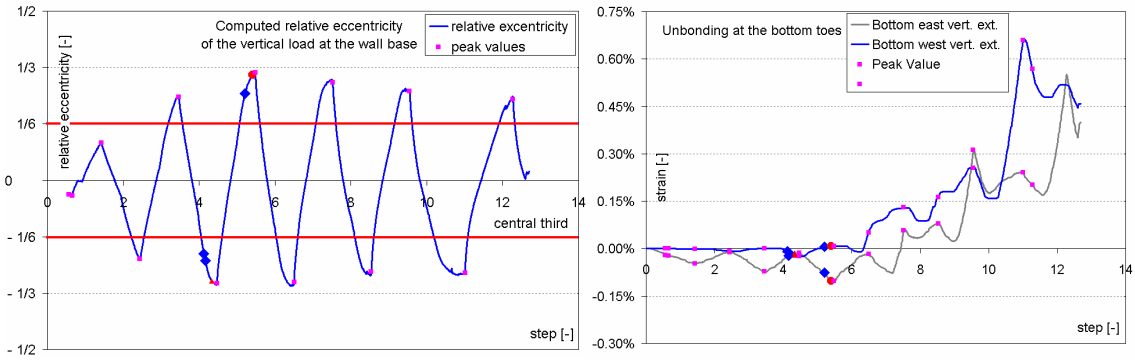

Figure 4: Relative eccentricity and toes unbonding strains versus load step.

The relative eccentricity of the vertical resultant at the base of the wall (see Fig. 4) has been computed using the following expression: $e = hH / 2BV$ where e, B and h are the eccentricity of the vertical resultant, the width of the wall (in its central part) and the total height of the wall. H and V denote respectively the horizontal and the vertical resultants applied by the upper-beam to the wall. Note that the proposed equation assumes that the vertical resultant is applied on the vertical symmetry axis and that the weight of the loading frame can be neglected with respect to the load applied by the jacks. The vertical resultant is out of the central third for all peaks following the 3rd one signifying, either some uplift of the base or, more probably, some tensile unbonding process in the toes area.

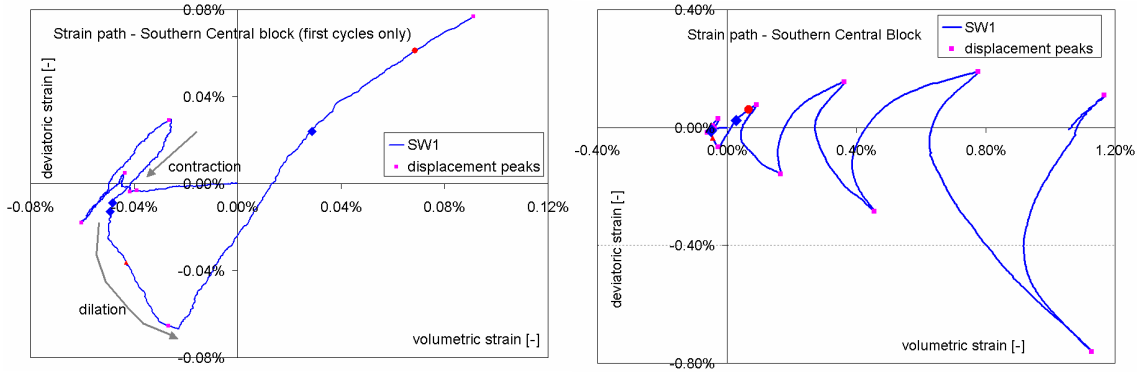

Figure 5: Deviatoric strain versus volumetric strain for the southern face.

The set of extensometers placed on the southern face of the wall (see Fig. 2) provides the following structural results. From the video recorded during the test, some lateral expansion caused by the cracks opening/closing is observed. Therefore, the volumetric changes versus the “shape” changes were understood to give a fair representation of the physical behaviour of the central part of the wall. Using set of extensometers covering the central part of the wall, the average volumetric strain has been determined on the basis of the results obtained on the four lateral extensometers, whereas the average “distortion” was found out with the two diagonal extensometers. Until the end of the 3rd displacement peak, the behaviour is basically contracting (up to a value of 0.06%) though an abrupt change occurs between the 1st and the 2nd displacement peak (see Fig. 5): no explanation has been found yet to give an accurate interpretation of such phenomenon. However, the main change occurs between the 4th and the 5th peaks: from an initially contracting phase, the behaviour gradually showed evidence of some dilation. It has to be underlined that the transition coincides with the occurrence of the first heard sonic emissions induced by units crack-

ing. Afterwards, the evolution of the volumetric strain versus the distortion follows successive recurrences of two stages: first, of contraction, then, of dilation (up to a value of 1.13% for the volumetric strain at the 11th peak), between each displacement peak. It has to be noticed that this behaviour is not symmetric with respect to the volumetric strain axis (see Fig. 5). Another sets of extensometers were fixed in the lower and upper parts of the southern wall (see Fig. 2) with the aim of checking the eventual unbonding of the toes. Though the results are not fully symmetric, the deformations are of the same order of magnitude concerning either the western or the eastern side (see Fig. 4). The lateral extensometers positioned in the central area always displayed contraction. Conversely, the extensometer located at the bottom and the top parts of the wall exhibited some expansion around the 8th - 9th peaks. It should be emphasised that the recorded tensile strains are much larger at the bottom than at the top of the wall. As expected, some unbonding process occurred since tensile strains were measured, it is problematical to define the "real" step of its occurrence. Indeed, the suspected initial closing of the defects may disturb significantly the analysis.

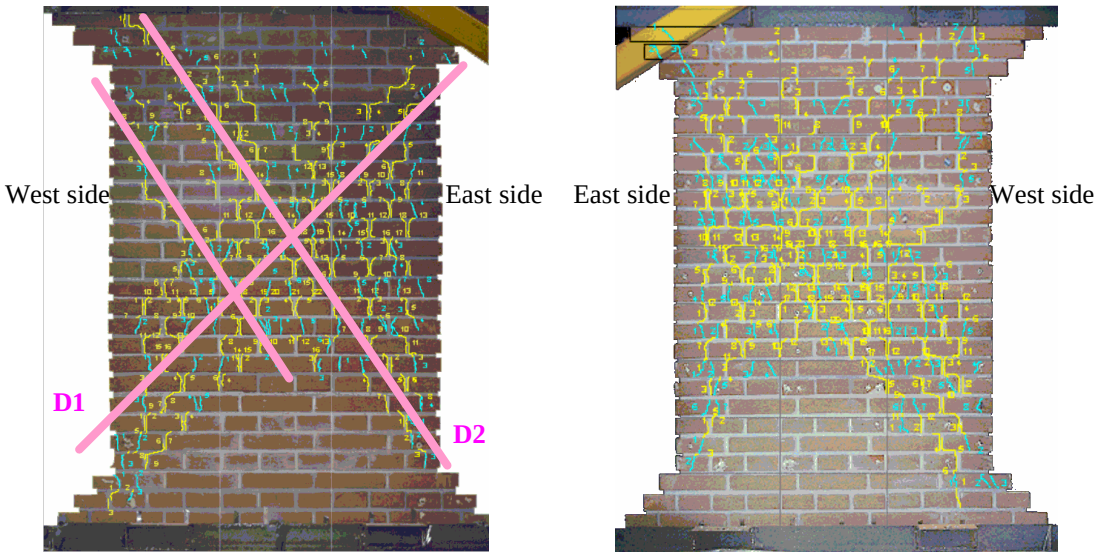

Figure 6: South (left) and north (right) crack pattern.

The crack patterns have been reckoned after the test. They are provided for the northern and the southern sides of the wall. The cracks have been distinguished for the two constitutive materials: the bricks and the mortar joints (see Fig. 6). The wall exhibited some effective damage both in the mortar joints and in the bricks. The crack patterns are not identical from one side to the other: the cracks seem more disseminated on the northern face. However, the pattern shows evidence of a large diagonal – called D1 for the sake of simplicity – cracking area of about nine units high, joining approximately the two diagonal opposite upper-east and lower-west toes of the southern side (resp. east to west on the northern side). The inclination of D1 with respect to the vertical is around 50 [deg]. In the following, the case of the southern side is detailed. There is also some damage in the diagonal – referenced D2 – joining the upper-west toes to the lower-east one but with a total lack of symmetry with respect to the diagonal D1. The diagonal D2 may be interpreted as two parallel slip bands going approximately along a line connecting the lower-east toe to the first western head joint of the upper brick layer. The inclination of D2 with respect to the vertical is around 30 [deg]. Another west-to-east diagonal was also created from the 21st layer. The eastern side showed also some large damage in the triangular area shaped by the diagonals D1 and D2 – it is mainly concerned with some vertical cracking/unbonding. As far as the northern side is studied, the previous conclusions seem to hold.. Qualitatively, the number and the dimensions of the cracks are comparable on both faces. However, the bricks cracks are 30% more numerous on the northern side and give a cumulated length 30% (resp. 37% for the width) higher on the northern side than on the southern side. The participation of the brick cracking in the dissipation process was estimated using the following expression $D = \int G_I^b d/2 \cdot dl$ where D, d and G_I^b are respectively the total dissipation induced by cracking, the depth of the wall and the fracture energy associated to the first mode of failure (tensile mode), and where the sum is performed

on both sides of the wall. It was found that the dissipation introduced by the formation of cracks within the brick does not exceed 5 to 10% of the total computed. It confirms that the dissipation was mainly induced by friction in the previously damaged joints and bricks.

The inclinometers were fixed on the bricks for different heights (see Fig. 2). The measured rotation may be induced both by a local motion of the unit, or by a structural effect (for instance, a curvature induced by some bending). It is precisely this second effect that is sought. The interpretation remains rather tricky since it is almost impossible to separate the local and global components.

2.2.3 Cell behaviour

Seven square periodic cells/blocks have been instrumented on the northern face of the wall (see Fig. 2). Four cells are symmetrically positioned in the four "corners" of the wall (related numbers: 1, 2, 6 and 7), three cells are located in the centre of the face (related numbers: 3, 4 and 5).

In order to obtain coherent/comparable results with those of the southern face, the strain path of each cell has been plotted in the previous frame *volumetric strain* vs. *distortion*. Wherever the cell is situated, the first displacement cycles induce only some volumetric contraction up to 0.085% in the 2nd block – top west cell –. Finding similarities between the different cells is an arduous task due to the discrepancy of the observed strain paths. Some correlations between the occurrence of the first cracking "noises" and a transition from a contracting phase and a dilating phase may be observed in the 7th block – bottom west cell –, and (with some more doubt) in the 1st block – top east cell –, and eventually in the 4th block – centre west cell – (see Fig. 7). Later, the strain paths progressively reach the dilation domain almost simultaneously between the 4th and the 5th displacement peaks for the 1st (top east), 3rd (central east) and 7th (bottom west) cells, between the 5th and the 6th displacement peaks for the 6th cell (bottom east), between the 6th and the 7th displacement peaks for the 5th cell (central), and finally between the 7th and the 8th displacement peaks for the 2nd (top west) and 4th (central west) cells. The behaviour within the dilating domain is much more regular than within the contracting regime. A distinguished analysis of the four corner blocks on the one hand, and the three central blocks, on the other hand, could be proposed. As far as the corner cells are concerned, their behaviour seems rather analogous though not fully symmetric. Along a complete "cycle", the cell exhibits once again some contraction/dilation behaviour.

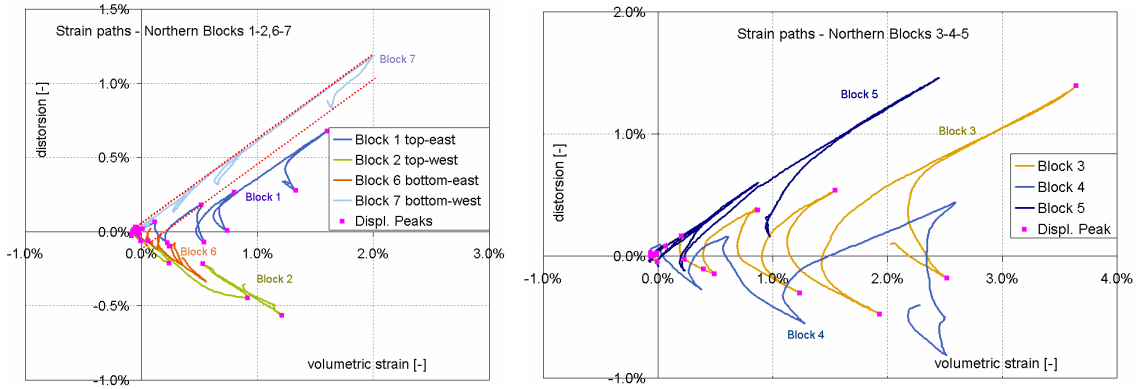

Figure 7: Strain paths for all the northern cells.

The behaviour of 7th cell – located at the bottom west toe – is detailed as a reliable example: the strain path is confined within a very thin band; the volumetric strain seems to act as an internal memory variable: when the previously attained maximum volumetric strain is exceeded, the strain path follows an almost straight line demonstrating that the ratio of the two principal strain rates is fairly constant (see Fig. 7). It should be underlined that the absolute value of the angle of the mentioned line seems almost independent from the position of the cell. The strain path induced by the succession of contracting unloading/dilating reloading, describes a thin loop that could be approximated by a simple linear trend. Such conclusion does not hold for the 1st block located at the top eastern corner where some "hook-shaped" path is more significant. Accordingly is the case for the strain paths of the central three blocks (see Fig. 7) that is found very similar to the one obtained with the larger central block on the opposite northern side (see Fig. 5). The volumet-

ric strains reach some ultimate values of 2.5% (4th and 5th cell) and 3.6% (3rd cell) at the 11th peak. The ultimate volumetric strains in the corner cells do not exceed more than 2.0% (7th cell) whereas the 6th cell has only recorded 0.6% (other maximum values 1.6% and 1.2% respectively for the 1st and the 2nd cell). Concerning the distortion, the values obtained with the corner cells and those obtained with the central cells belong to some similar range ([-0.6% ; 1.2 %] for the corner blocks, [-0.8% ; 1.4 %] for the central blocks).

Finally, the orientation of the principal strains has been computed for each northern block. It has to be emphasised that the computed principal strain directions are very sensitive with respect to small deviation of the measured strains. Some poor correlation has been found among the sets of data corresponding to the same cell, though some pairs of extensometers may be often related. Nevertheless, two exceptions shall be discussed in some more detail: the 2nd block (top west) and the 4th block (central west). As far as the 2nd block/cell is discussed, some quite fair correlation may be established between the four series resulting from the analysis of the four triplets of extensometers intersecting the corner cells. After the 7th peak, the trends of the four series are very similar and seem to reach some "yielding" values. The computed orientations of the principal strains seem no more affected by the changes of sign of the upper-beam horizontal displacements. This result has, of course, to be compared with the corresponding strain path (see Fig. 7) that exhibits some almost continuous increase of the volumetric strain without changing the sign of the distortion. The resultant "yielding" values are found between 5.0 [deg] and 21.7 [deg]. Though the interval is undeniably too wide to quantify the final orientation of the average principal strains, the consequent range gives an estimation of good quality about the post peak behaviour of the wall: it supports indeed the idea that the compression struts evolve from a toe-to-opposite toe diagonal to a pair of redressed split struts in the post peak regime.

2.2.4 Local measures

Two horizontal lines respectively of 3 and 4 extensometers were fixed in the centre of the northern face (see Fig. 2). The objective was to acquire some information about the brick cracking/mortar head joint unbonding process. The occurrence of the brick cracks are clearly tracked since they produce a sudden increase of the elongation in the cross direction. The first sonic emissions trigger a high gradient of the measured data of the lower west central and upper central extensometers. A lower, though effective, gradient is observed in the lower east central and the upper east end extensometers, so that it shall be concluded that the first brick cracks, at half of the wall height, appear in the centre of the wall. The further sonic emissions are also correlated with three events: *(i)* a high gradient in the lower east central and the upper east end extensometer suggesting some further opening of the pre-created cracks, *(ii)* the splitting of the histories recorded in the lower west central and the upper central extensometers – up to that point, they were fully correlated, *(iii)* the initiation of a strong increase of the tensile strain in the lower east end that almost balances the previous – see item *(ii)*.

2.2.5 Interpretation and conclusion

From the previous observations, the behaviour of the wall shall be interpreted as follows:

- The vertical pre-loading has induced a closing of the existing defects (unbonding due to high shrinkage).
- The cyclic horizontal displacements with increasing of the peak-to-peak amplitude have developed two successive stages of the wall behaviour. Until the 4th peak, the wall exhibited some slightly non-linear behaviour probably induced by opening/closing mechanisms of the unbonded joint/mortar interfaces. The unbonding process is induced by some cyclic damage. Before reaching the 5th peak, cracking of the bricks occurred in the central part of the wall. The origin of the tensile failure in the bricks has not been clearly discriminated by the instrumentation. However, it seems to be induced by some local bending of the bricks (this result is confirmed by the numerical simulations). The brick failure initiated gradually a failure mechanism by developing some diagonal stripes connecting the brick cracks and pre-unbonded mortar/unit interfaces. The crack openings induce a lateral expansion of the wall (the so-called "bulking" or "barrel" effect). The crossed-diagonals form a stable and highly dissipative failure mechanism.

Though, the test did not investigate the behaviour induced by larger horizontal displacements than 20 [mm], it seems that the loss of strength capacity is minor. The relative eccentricity (with

respect to the vertical resultant below the wall footing) computed for the horizontal displacement peak values, decreases very steadily (from 0.27 to 0.25 with respect to the four latest peaks). If it is reckoned that observed failure mechanism is stable, then the value of ¼ for the final relative eccentricity could be used as a design value. The numerical simulation confirms that the final compression strut may be geometrically obtained by tracing a straight line joining one of the upper toes to the centre of the base.

The wall exhibited some unexpected ductility. The maximum prescribed horizontal displacement reached up to 20 [mm]. Two main reasons may be addressed to explain such result:

- The materials used in this specific project – porous solid clay brick and lime mortar of poor quality – are relevant of ancient masonry buildings and thus, the consequent behaviour should not be compared with modern/industrial masonry made on brittle hollow units and cement mortar. As mentioned by Sofronie (2000), the increasing strength implied by the use of such materials has for corollary that recent masonry has *almost completely lost its ductility*. It shall also be underlined that this ductility has provided some self-defence for the historical/ancient building/monuments against differential settlements, natural hazards or technological aggressions.
- The boundary conditions provided by the experimental set-up are favourable to create a structural ductile behaviour. Since the vertical displacement of the upper-beam is released, no increasing of the vertical confinement is induced. Once the diagonal splitting of the wall is reached, a "four triangular pieces" closing/opening mechanism is created. This mechanism is highly dissipative since it provokes dry frictional dissipation within the unbonded mortar/units interfaces and the existing cracks within the bricks. Though the failure mechanism has been reached, the wall is still highly stable. The loss of residual strength for the horizontal mode seems rather small and large displacements can be ensured. Conversely, if the vertical degree of freedom is fixed (see for instance the results from the CUR Project (1994)), then a brittle failure concomitant to a large increase of the vertical load may be observed for small displacements (around 3 [mm]) especially when the vertical confinement becomes far too important (around 2 [MPa]). However, Lourenço (1996) mentioned *that the walls behave in a rather ductile manner, which seems to confirm the idea that confined masonry can withstand substantial post-peak deformation with reduced loss of strength*.

2.3 Further testing campaign

The results obtained on SW1 allowed first to access the convenience of the testing setup.

At the level of the instrumentation, some limitations have been found. First, the inclinometers do not furnish valuable results and it was decided to rotate them in order to obtain some indication about the out-of-plane behaviour of the wall during the following tests. Second the most complex arrangement of "self stable" transducers does not furnish more precise informations at the cell level and it was decided to rely only on the simple arrangement for the tests needing local cell measurements.

In order to precise more accurately the behaviour of the wall, two other tests on the bare structure (without reinforcement) have been programmed: a monotonic test up to failure (SW2) and a test involving series cyclic loading (three cycles) of increasing amplitude in each zone of the damage diagram (SW3).

Since it is difficult to compare retrofitting techniques (the initial damaged structures should be identical as much as possible, injection is almost always required), it appeared to be easier to reinforce the walls and to subject them to the same cyclic history as SW3. Three types of reinforcement, applied on each side of the wall, will be first considered: glass fibre reinforced mortar (SW4), steel fibre reinforced mortar (SW5) and carbon composite (SW6).

3 WALLETTE

3.1 Test setup and instrumentation

A special testing rig has been designed for the purpose of the tests, which consists of loading biaxially the wallettes, keeping it homogeneous as much as possible. The square specimen is placed horizontally between four steel plates (see Fig. 8). Each pair of opposite plates can be moved by

means of four actuators working by couples in two horizontal layers. Each piston in the same couple delivers the same force and can be controlled by means of a common displacement transducer connecting the opposite plates in their vertical centre plane. Four displacement transducers are thus present, two under the wall and two over it. In order to smooth local surface heterogeneity and to allow the wall to move along the plates, teflon sheets are introduced at the boundary between the wall and the plates.

Note that this setup would allow the plate to rotate around the vertical direction in the case where directions of anisotropy of the masonry do not coincide with the ones of the loading. Note also that the orientation of the principal axes of anisotropy for the wallettes are to be determined with respect to the observed principal directions in significant regions of the shear wall (for instance main strut orientations). The load histories have also to be specified as close as possible to the ones experienced by the different parts of the shear walls.

Some reference tests– axes of anisotropy and loading direction coincide – are first performed to validate the setup.

The instrumentation has been conceived in order to check the periodicity of the behaviour and to obtain indications about local side effects.

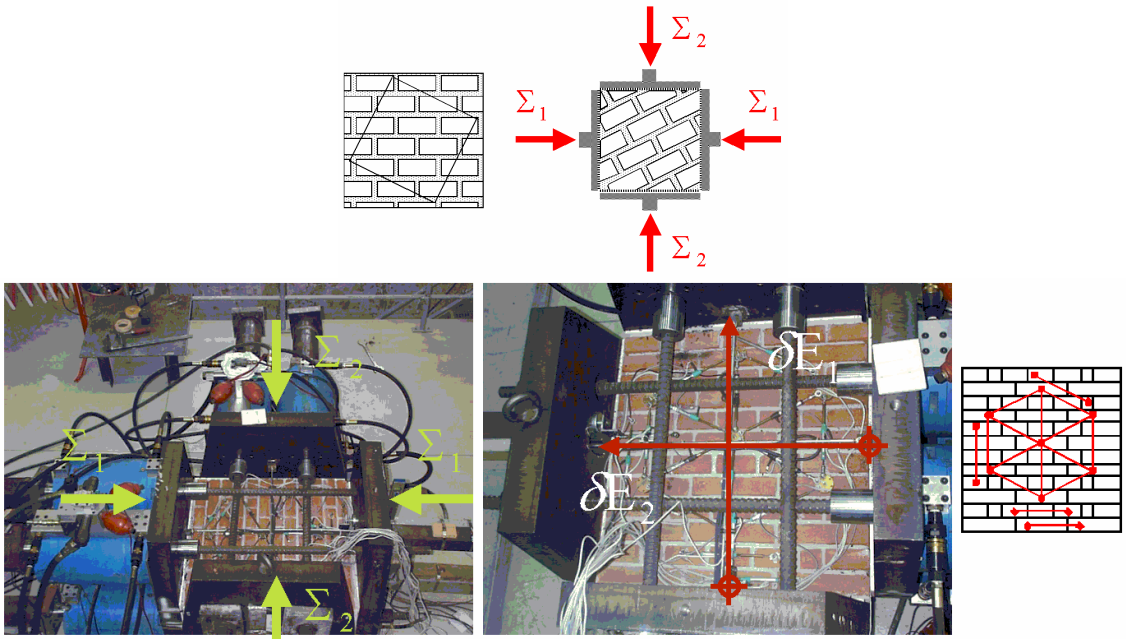

Figure 8: Test principle, setup and instrumentation for the wallette.

3.2 Results observed during the first test.

The first test was mainly devoted to checking the operability of the loading control.

3.2.1 Loading

The foreseen loading was the following: (first step) apply a confinement force of 50 [kN] on all the sides of the wall, (second step) perform a compression loading/unloading cycle controlled in displacement in one direction while keeping the force in the other direction equal to 50 [kN], and (third step) perform the same compression cycle, permuting the loading directions.

3.2.2 Problems observed during the test

The test has been faced with one main problem implying some improvements of the loading control. In fact for this test, the two horizontal layers of actuators in one direction were not coupled together when a force had to be imposed or kept constant. For instance, during the first step each layer was asked to deliver a force of 25 [kN]. Unfortunately a side of the wall were slightly damaged along its depth so that the plates applying the load in the direction 2 (see Fig. 8) did not succeed to remain vertically parallel. The effort made to correct manually this problem introduced further damage at the interface resulting in a more pronounced rotation of the plates.

At this point it was decided to perform the loading with the existing control, knowing that the in-plane character of the loading was not ensured. In fact the wall bended gradually out of plane. The second step was displacement controlled along direction 2 and some bricks were expelled out-of-plane during the last step displacement controlled in direction 1, although no softening was observed in the force displacement curve (see Fig. 8).

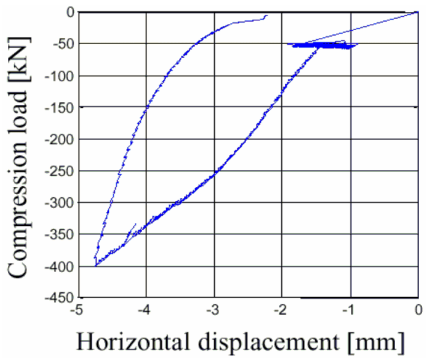

Figure 9: Load/displacement curve along direction 1.

3.3 Further work

The further work for the wallettes will concern first the update of the setup. Apart from building a more rigid loading apparatus, where the plates are forced to remain vertically parallel, it seems that the most easier solution is to increase the capacities of the control when a force is imposed: like for the vertical motion of the wall, the sum of the horizontal forces to be delivered by the two layers of actuators in one direction would be specified and its effective transfer to the wallette would be performed in such a way that the motions of the top and bottom displacement transducers remain equal.

After the validation of the setup, the practical problem of the preparation of the wallettes with inclined bed joints will be faced. What is foreseen is to cut a larger wall in the chosen direction as sketched in Fig. 1.

4 CONCLUSIONS

An overview of the experimental work performed within the framework of the SEISPROTEC project was presented.

The test setup for the masonry walls performed rather well and the results that have been obtained on the first wall, at the global, cell and local levels, have been presented and commented. The further test campaign, currently in execution phase, has also been outlined.

The test setup for the wallettes, in its first release, was not able to guaranty the in-plane nature of the loading. Some improvements of the control procedure are underway to fix this problem.

5 REFERENCES

CUR 1994. Structural masonry: a experimental/numerical basis for practical design rules (in Dutch). Report 171, CUR, Gouda, The Netherlands. Also quoted in Lourenço (1996).

Le Pape, Y., Anthoine, A. and Pegon, P. 2001. Seismic Assessment of Masonry Structures – Multi-Scale Numerical Modelling. *These Proceedings*.

Lourenço, P.B. 1996. Computational strategies for masonry structures. Ph.D. thesis of Delft University of Technology, Delft University Press.

Pinto, A. Molina, J., Pegon, P. and Renda, V. 2001. Protection of the Cultural Heritage at the ELSA Laboratory. *These Proceedings*.

Sofronie, R.A. 2000. Geogrids for reinforcing masonry buildings and structures. *In Proc. of the 2nd European Geosynthetics Conference & Exhibition EURO-GEO, October 15-18, Bologna, Italy*, pp. 847-852.